CB Note 341

A New Photon Energy Correction Function and the JDC z-Scaling for Inflight Data

I. Uman, O. Kortner
University of Munich

October 30, 1998

1 INTRODUCTION

The present note will show the results of a new photon energy correction function that can be used either for data at rest or in flight. The results are compared with the correction function that was used by Hessey [1] and subsequently adjusted by Schmidt for in flight data. The documentation describing the correction from Schmidt is not available and the procedure is only shortly described in the software. For this reason and for the fact that several groups working in flight found a non-negligible missing momentum, as compared to the value of the antiproton beam from LEAR, we tested again the calibration at higher photon energies.

The second part of the note concerns the JDC calibration. A correction that takes into account also the new resistive wire length scaling for the JDC describes properly the data with PEDs and charged tracks in the final state [2] [3].

2 PED Energy Correction

2.1 MC Simulation of Single Photons

The Photon Energy Correction Factors (PECF) are defined to give the best estimate of the photon energy, given the energy of the PED (Particle Energy Deposit), E_{PED} and the position of the photon.

$$E_\gamma = f(E_{PED})C(\theta)E_{PED}$$

In Hessey's work 6 photons were generated from $\bar{p}p$ annihilation at rest and the correction is separated into energy dependent and θ dependent parts by plotting PECF $= E_\gamma/E_{PED}$ against E_{PED} to get the energy correction function and by plotting PECF versus θ to get the correction factors for different crystal types.

The crystal type 13 and the crystal type 0 show the highest energy losses because of the holes and the aluminium plates.

At higher energies the shower size is roughly independent of the energy of the photons, so we assume that the angular correction is exact.

To check the energy behavior we wanted to have the simplest configuration. We generated a single photon isotropically distributed over the sphere at different energies (CBGEANT version 3.21/05). The generation is done, again for simplicity, with a fixed vertex at the center of the Barrel. The reconstruction of these events has been done by removing the energy dependent correction and keeping the angular one. The usual cut at 20 MeV for PED equivalent to what is used for data in flight to remove events with split-offs was used and no type 13 PED for the central crystal. Here we show some significant points (fig. 1). The distribution of the total energy shows a big tail at high generated $\gamma-$energies that give us an indication that for in flight data the mean value of the response cannot be taken to get the correction function. For this reason we take the peak to get the response. Namely we perform a gaussian fit limiting ourselves to a region close to the peak.

The result is a linearity of the PED energy of the photons even at high energies (fig. 2).

The relative highest energy losses are at the lowest photon energies. This energy loss persists also when we use lower threshold energies for the crystals (DSTP 1).

We also plot N. Hessey's PECF. It is a cubic function up to 250 MeV and a straight line for $E_{PED} > 250$ MeV. It agrees within 2 σ up to photon energies of about 900 MeV which is the phase space allowed limit for data at rest. Schmidt makes an additional correction to the big energy losses (the correction are applied to the cluster energy) in flight. The default correction applied (namely Schmidt and Hessey) are also shown. From our simulation their PEFC is not satisfactory for gammas of an energy higher than 1300 MeV.

In first approximation, one can use a constant correction factor of PECF=0.99. However, due to the deviations from it at low photon energies, one has to take a higher order polynomial in E_{PED} as correction function. Our best fit, a cubic polynomial, similar to Hessey function, up to 200 MeV and a constant factor of 0.99 for higher energies, is shown in the same figure. Apart of this small deviation at low energies we can say that the E_{PED} is linear and the correct energy level of the crystals can be obtained optimizing the PECF with a multiplicative factor to get the right π_0, η and ω masses.

An additional test of the energy response assuming a flat vertex distribution in z-direction of the photons along the target, that better simulates the displacement of the vertex for annihilation in flight, does not show a visible energy shift. In this case, during the reconstruction, the vertex z coordinate is shifted from the center to -0.45 cm. The energy spread i.e. the width of the gaussian is increasing but the peaks are shifted only by 0.2% (fig. 3).

2.2 MC Simulation of $\bar{p}p \to \eta\pi^0$ Events

The π^0 is not a good candidate to calibrate the crystals at high energies because the invariant mass shows different values at different π^0 energy intervals. The reason of this non-linearity can be explained taking in consideration that at high energies PEDs can even overlap for asymmetric π^0 decays; for these cases the angle determined between the PED-maxima are smaller than the angle between the photons.

In fact the angle between the two photons is related to their energy E_1, E_2 according to the

$$m^2_{\pi^0} = 2E_1E_2(1-\cos\psi) = 4E_1E_2sin^2(\psi/2)$$

where ψ is the angle subtended at the decay vertex in the lab system. In the fig. 4 we plot this angle in function of the π^0 energy.

At different ranges of the ψ angle, namely for $cos\psi < 0.95$ and for $cos\psi > 0.95$, the relative difference in the π^0 mass is $\Delta m_{\pi^0}/m_{\pi^0} = 5.1/135 = 0.038$ (fig. 5).

The η with a higher mass decays with a higher angle between the two gammas and has an invariant mass that is almost constant and consequently gives a better check of the calibration (fig. 6).

For $cos\psi < 0.55$ and for $cos\psi > 0.55$, the relative difference in the η mass is in fact only $\Delta m_\eta/m_\eta = 3.8/547 = 0.0069$ (fig. 7).

To compare MC with one of the last runs in flight we generated 20000 events for the $\eta\pi$ final state at 1642 MeV/c. Again usual cuts at 20 MeV, no type 13 PEDs for the central crystal, and events with only 4 golden gamma were selected. Here we define as "golden gamma" event a PED which has an energy of the central crystal higher than 13 MeV and an E_1/E_9 ratio less than 0.96.

The usual definition of golden gammas with the additional split-off recognition with DOLBY C and the subsequent correction has not been used. The reason is again that the merged photons from decaying particles (η's or π^0's) at higher energies overlap with the split-offs. The DOLBY C routine [4] can separate split-offs from photons up to a maximum energy of the π^0 of 950 MeV that is largely exceeded at 1642 MeV/c.

In order to get the invariant masses we do not make the kinematical fit. This process pushes the four vectors to the correct position giving us no indication of the quality of the calibration.

With only four gammas in the final state only three combinations of the four gammas, taken two by two, exist. When we plot all of them and we make an initial broad cut on the π^0 mass to reduce the combinatorial background, the remaining two gammas give the invariant mass of the η. In the fig. 8 we plot the invariant mass of the η, which has been obtained with different PECF of the crystals. The first plot shows that the η mass is around 543.6 MeV. In this case the default crystal correction has been used, namely the Hessey and the Schmidt correction. Removing all the corrections, that is PECF=1.0, gives the best result.

The η mass shift to 548.3 MeV is in a better agreement with the value of 548.8 MeV that is simulated from CBGEANT.

2.3 Selection of $\bar{p}p \to \eta\pi^0$ Events at 1642 MeV/c

About 5 million events of data at 1642 MeV of one of the last runs of NOV '96 have been reconstructed with the some cuts in the crystals as in the previous MC. Again no kinematical fit has been performed and a broad π^0 window cut has been done to reduce the background. The reconstruction with the default corrections gives a total momentum of about 1588 MeV/c, 54 MeV/c less than the nominal value (fig. 9).

Besides of our PECF function an additional correction factor of 1.007 for the PED energy is required to get the right m_η at about 547.1 (fig. 10). The reason of the remaining discrepancy of PECF= 1.0 and PECF= 1.007 that is 0.7% between our MC and the experimental data is not clear: this can be either because of split-offs or because of an incorrect single crystal calibration. This discrepancy is low and can be easily adjusted by the fitter, if this additional correction is not performed.

The π^0 mass is also consistent with this PECF: $m_{\pi^0} = 131.9$ MeV if $cos\psi > 0.95$, $m_{\pi^0} = 135.6$ MeV if $cos\psi \leq 0.95$ (fig. 11).

Furthermore the momentum loss is reduced from 54 MeV/c to 12 MeV/c (fig. 12). This improvement may be taken as main justification of our new procedure.

As an additional check we also show the ω mass with the $\omega \to \pi^0\gamma$ selected from $\bar{p}p \to \omega\pi^0$ events, that is data with 5 golden gammas. The shift from 768.4 to 775.9 MeV shows as well better agreement with the PDG value of 781.9 MeV, but the value is not accurate because of the high combinatorial background. (fig. 13).

3 Electrical Wire Length Scaling of the JDC

The correction of $tg\lambda$, equivalent to the scaling of the electrical wire length of the JDC, has been suggested at the CB meeting [2] and done by Heinzelmann [3].

The position of the hit along the wire is given by

$$z = z_0 + z_l(A_l - \alpha A_r)/(A_l + \alpha A_r)$$

where
z_0 = center of the signal wire
z_l = electrical wire length
α = correction of the preamplification signal of the individual wire
A_l, A_r = left and right signal amplitude

In this work, where he is matching the PED with the JDC, he proves that the factor z_l has to be increased by 6%. An additional estimate of z_l can be obtained analyzing the $p\bar{p} \to \omega\pi^0$ in flight, where the ω mass is decaying in $\pi^+\pi^-\pi^0$. The final state consist of 2 tracks and 4 gammas.

The reconstruction of one run of DEC '96 at 1642 MeV/c with 2-prong has been done. Again no kinematical fit has been performed and a broad π^0 window cut of the two pions has been done to reduce the background. Obviously, we removed the Hessey and Schmidt energy dependent correction and applied our correction of the crystal energy.

Here the $\pi^+\pi^-\pi^0$ invariant mass shows that the ω peak is shifted from the value of 771.4 MeV to a value of 779.0 MeV closer to the PDG value when the scaling is +6.5% in agreement with the value obtained from Heinzelmann (fig. 14).

4 USER's GUIDE

We list the subroutines referenced.

+PATCH,//BCTRAK/BCPHYS
+DECK,BCPEDS.

The Schmidt's cluster energy correction can be simply removed replacing

EC = Q(JTBTK+13)/(ECA*Q(JTBTK+13)+ECB)

with

EC = Q(JTBTK+13)

Hessey correction's are in

+PATCH,//BCTRAK/BCPHYS
+DECK,BCEGAM.
FUNCTION BCEGAM (ENER, ITHE)
Arguments: (INPUT,OUTPUT,INPUT/OUTPUT)
Expected input:
ENER = Energy of PED
ITHE = theta number of center of PED crystal
Final output:
BCEGAM = Corrected gamma energy

The original correction from Hessey that has to be removed is

```
IF (ENER .LT. E0) THEN
BCEGAM = ((A + B * ENER)/(A + B * E0) +
C/(A + B * E0) * (E0 - ENER)**3 ) * ET(ITHE) * ENER
ELSE
BCEGAM = (A + B * ENER)/(A + B * E0) * ET(ITHE) * ENER
END IF
```

our correction is provided by the parameters:

```
REAL A1,B1,C1,D1
PARAMETER (A1 = 1.013, B1 = -0.1858E-03 , C1 = 0.1137E-06)
PARAMETER (D1 = 0.1064E-8)
REAL PECF
```

Our fitted PECF is:

```
IF(ENER.LE.200.) THEN
PECF = A1+B1*ENER+C1*ENER**2+D1*ENER**3
ELSE IF (ENER.GT.200) THEN
PECF=0.9891
ENDIF
```

The PECF needs additional different factors: for MC

```
PECF=PECF*1.011
```

while for experimental data

```
PECF=PECF*1.018
```

The output PED energy BCEGAM is:

```
BCEGAM=ENER*PECF*ET(ITHE)
```

The JDC correction of the electrical wire length is easily done performing again the reconstruction with the following input card in FORT99:

```
CHAM 'TRAK' 'RTRK' 'RAWS' 'PATT' 'CIRC' 'HELX' 'VERT' 'GVTX'
'FFUZ' 'BXZS'
```

where the new scaling factor BXZS of 1.065 is given in the file FORT81=jdc.card

BXZS 1.065 1.00

5 CONCLUSION

The final kinematical fit with the present corrections shows better pulls and flat confidence levels, for all the channel taken in consideration, and consequently rises the number of events passing the confidence level cuts. We show here the pulls obtained with our corrections in the final $K^+K^-\pi^0$ final state at 900 MeV/c (fig. 15).

In particular with the JDC correction the pull for $tg(\lambda)$ is now centered as compared to the default corrections (fig. 15f, 16f).

The pull of the energy is also centered (fig. 15e, 16e).

Furthermore in a preliminary partial wave analysis of the $K^+K^-\pi^0$ final state the optimization of the $\phi(1020)$ mass, which decays in K^+K^- gives the result of 1019.2 ± 2.MeV where the PDG value is 1019.4. Without JDC scaling the optimum was reached at 1015 MeV.

References

[1] CB note 161.(26.06.91) N. Hessey, Photon energy correction factors, derived from response means.

[2] Minutes of the CB meetings. (01.98) Ismail Uman, $p\bar{p}$ annihilation into three body final state of charged kaons at 900 MeV/c.

[3] CB note 328. (05.98) Matthias Heinzelmann, Missing momentum of charged particles at 900 MeV/c and resistive wire length scaling.

[4] CB note 199.(28.08.92) N. Hessey, Split-off Recognition with Dolby-C

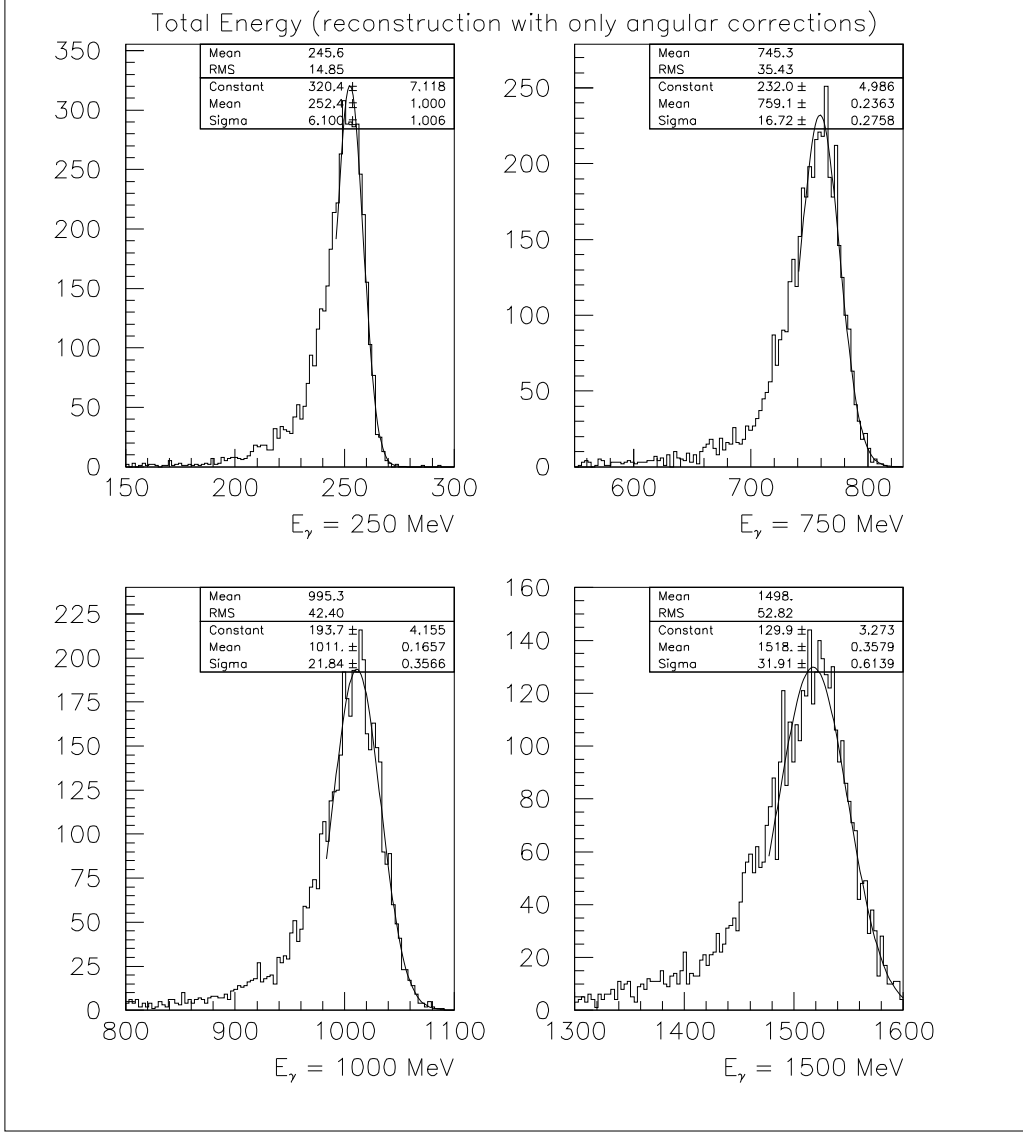

Figure 1: Energy distribution of reconstructed single photon MC events

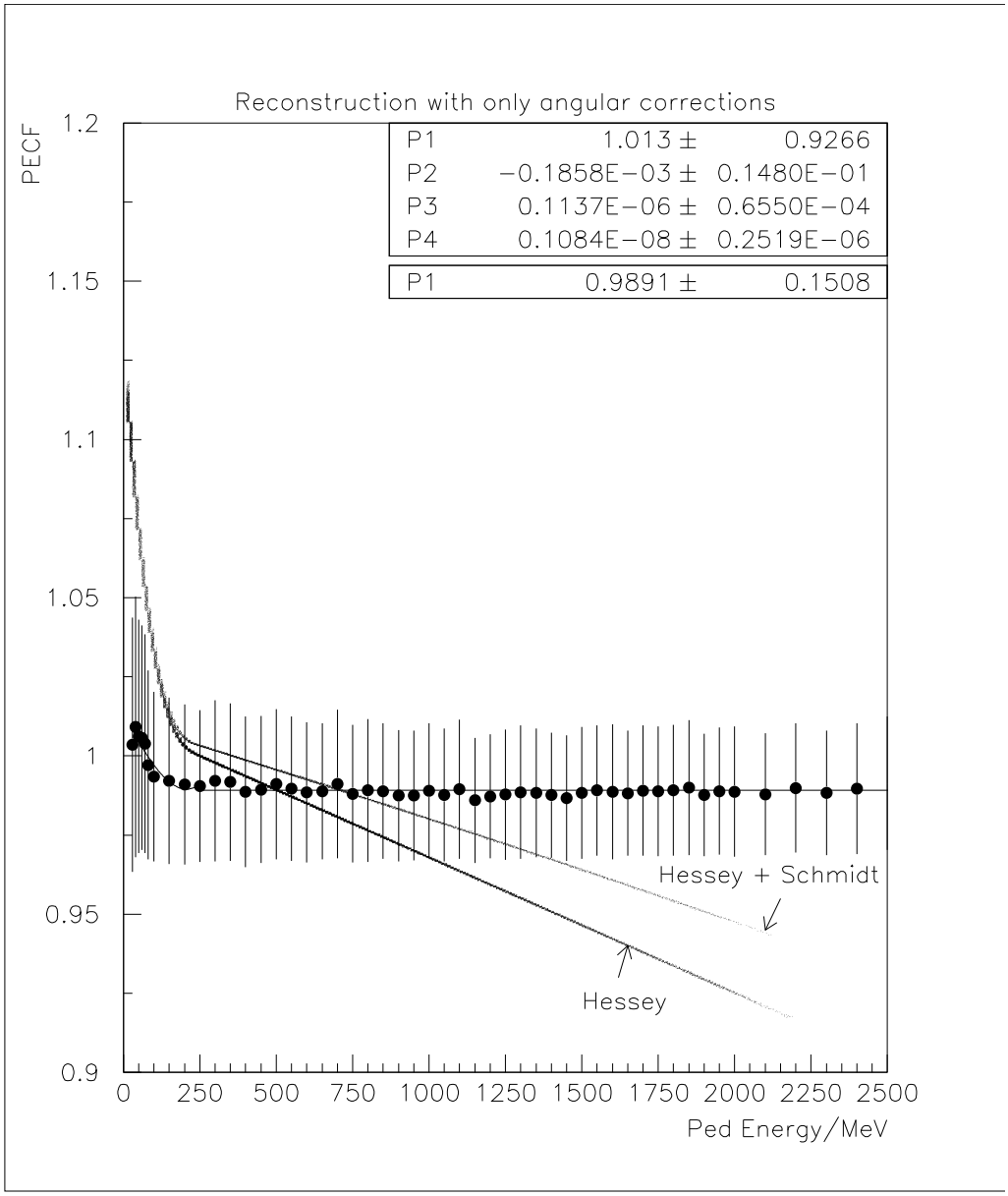

Figure 2: Photon Energy Correction Functions

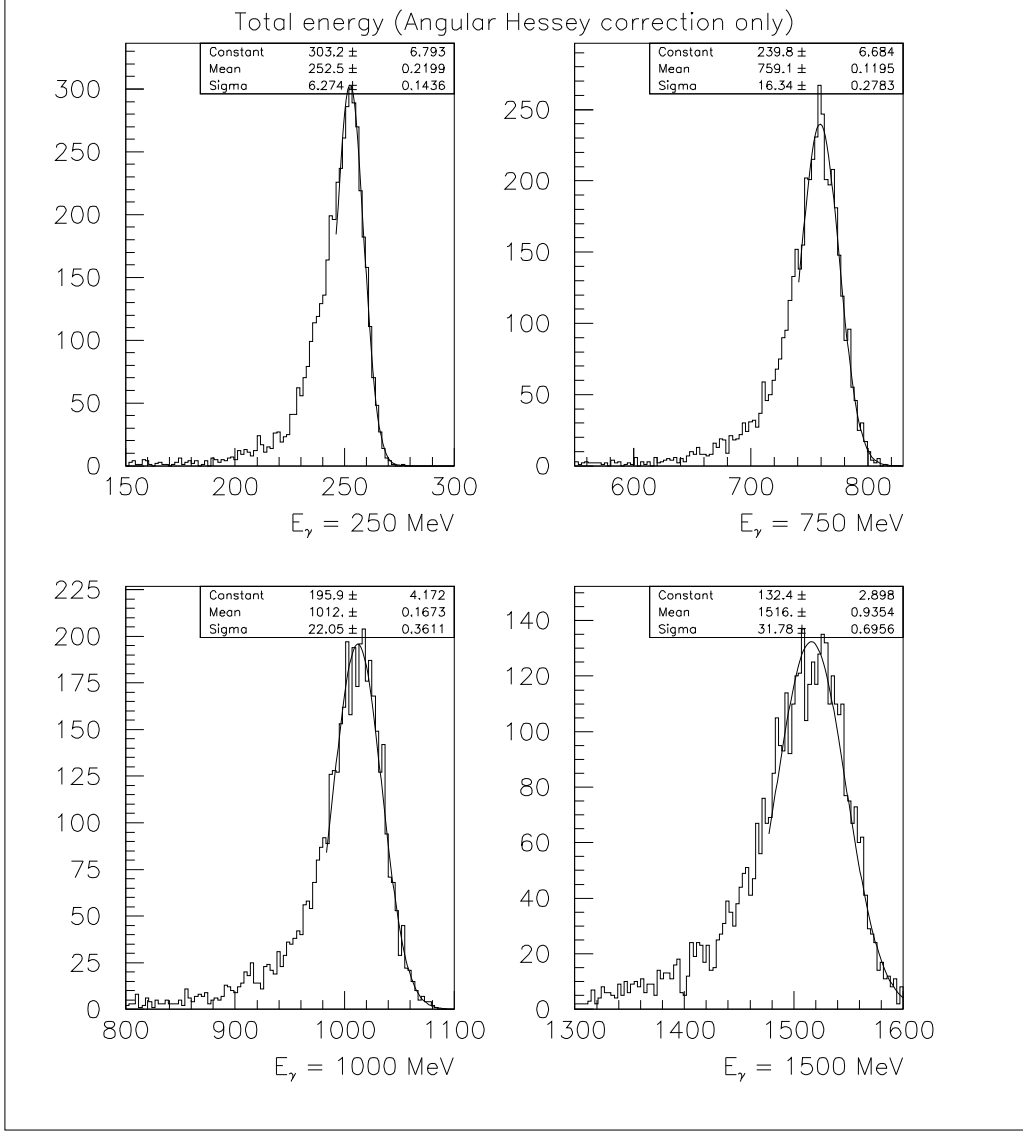

Figure 3: Energy distribution of reconstructed single photon MC events with a flat vertex distribution along the target

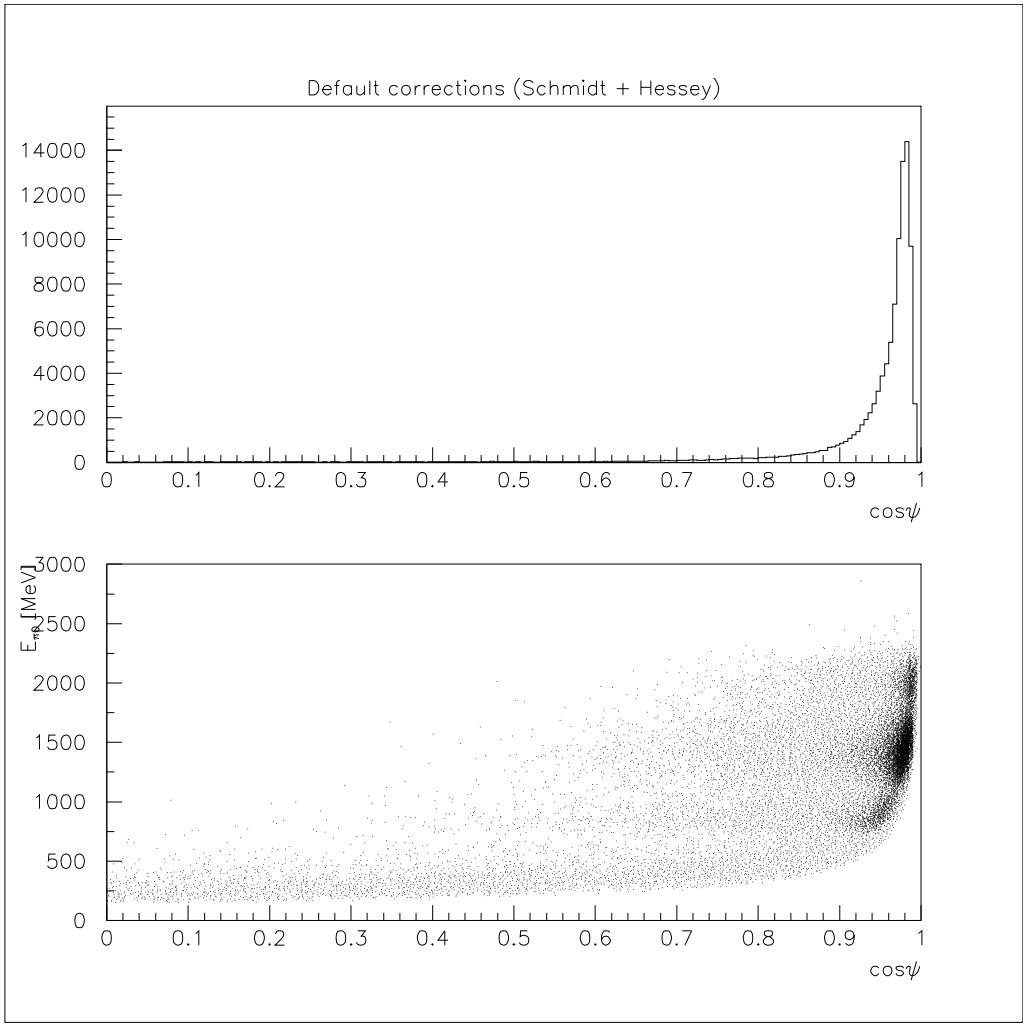

Figure 4: a) Distribution of decay angles at the vertex of $\pi^0 \to \gamma\gamma$ b) π^0 energy versus the decaying angle

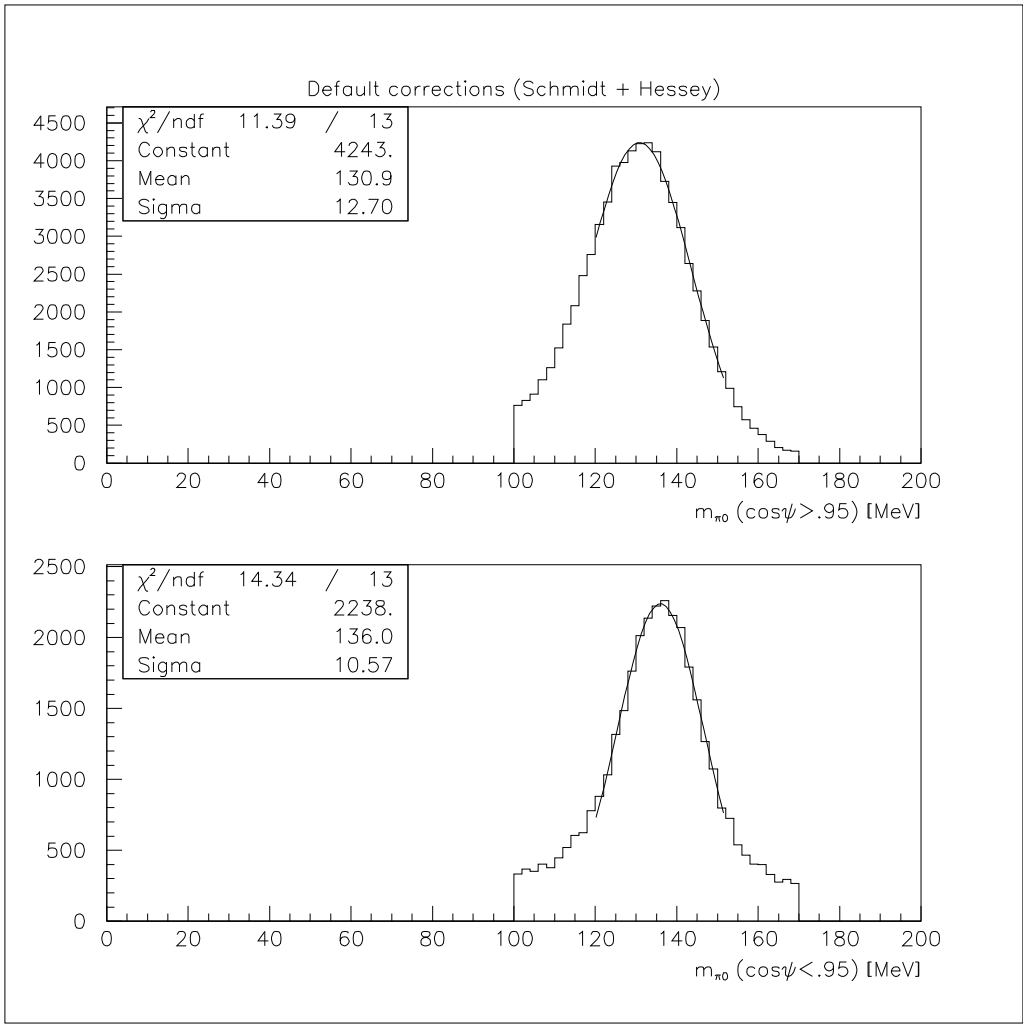

Figure 5: Invariant π^0 mass at different ranges of the decaying angle

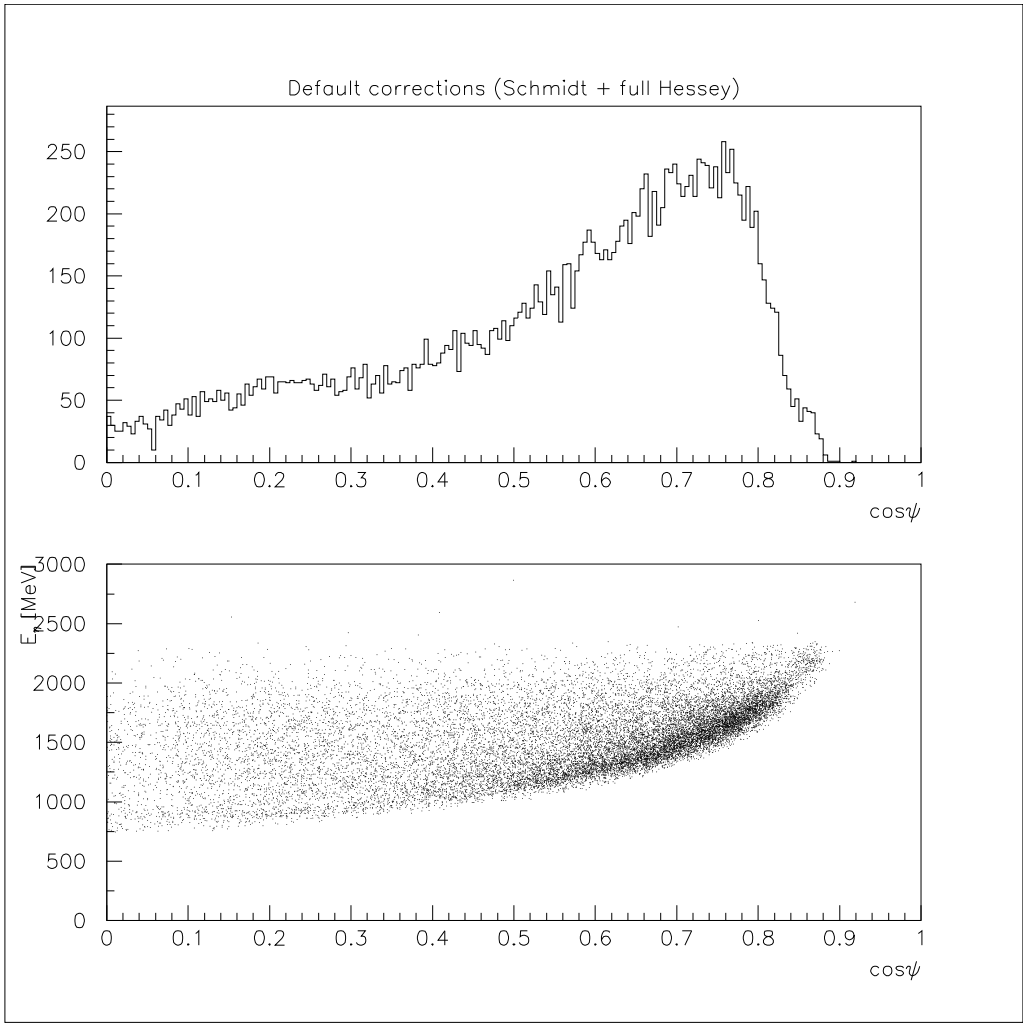

Figure 6: a) Distribution of decay angles at the vertex of $\eta \to \gamma\gamma$ b) η energy versus the decaying angle

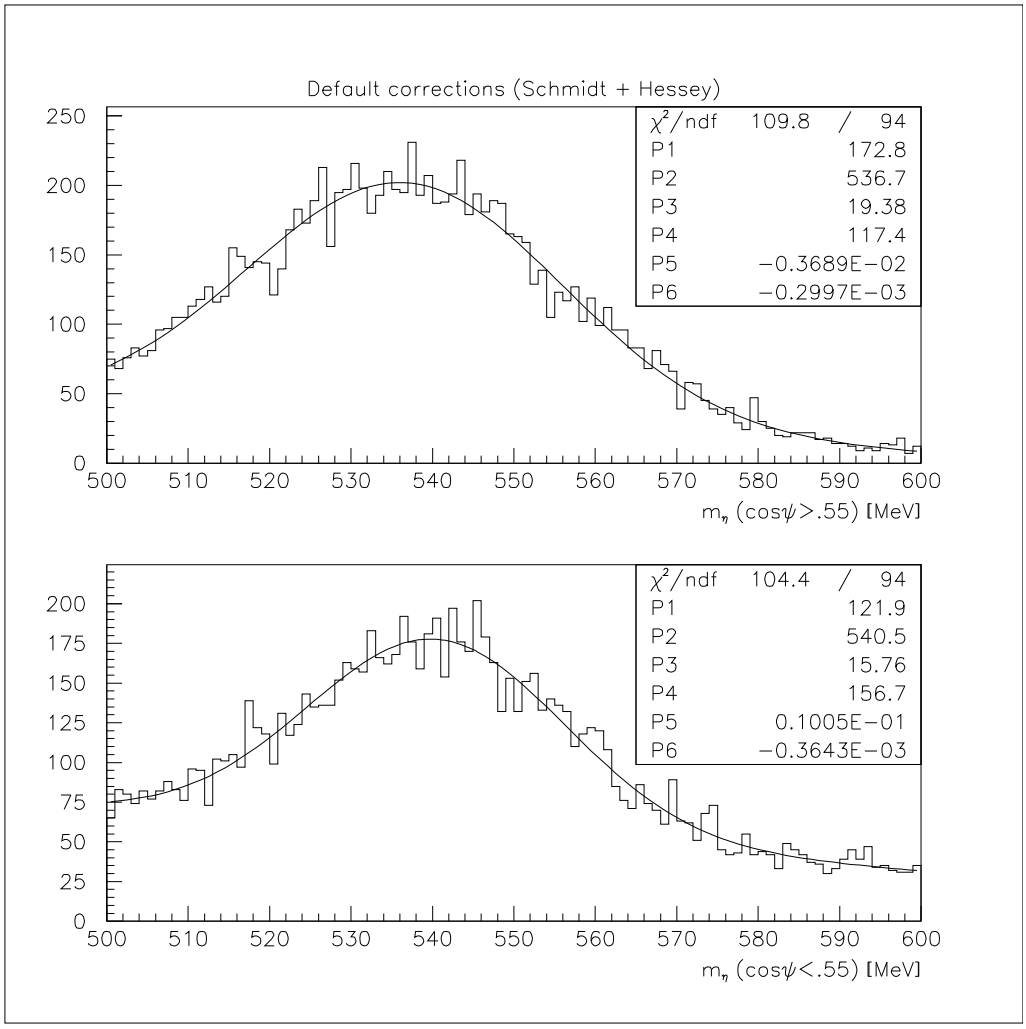

Figure 7: Invariant η mass at different ranges of the decaying angle

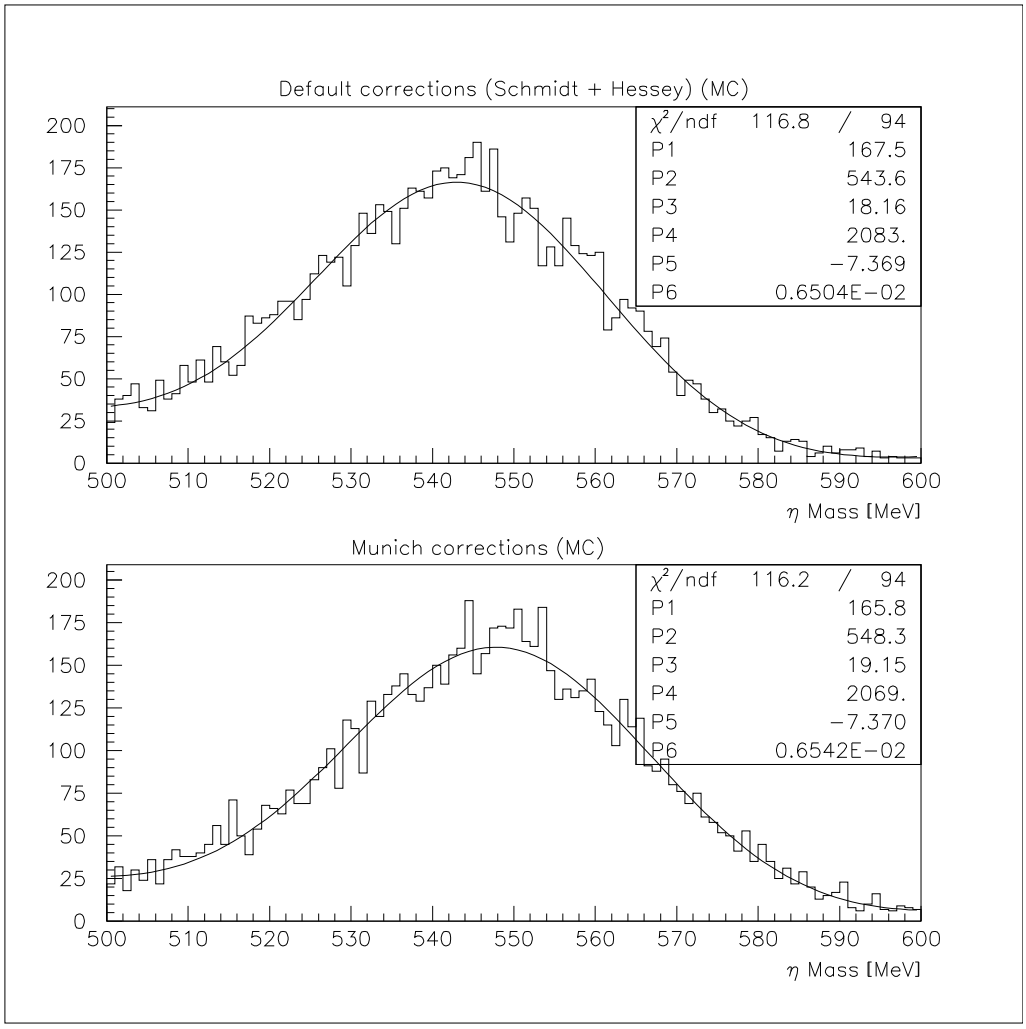

Figure 8: Invariant η mass

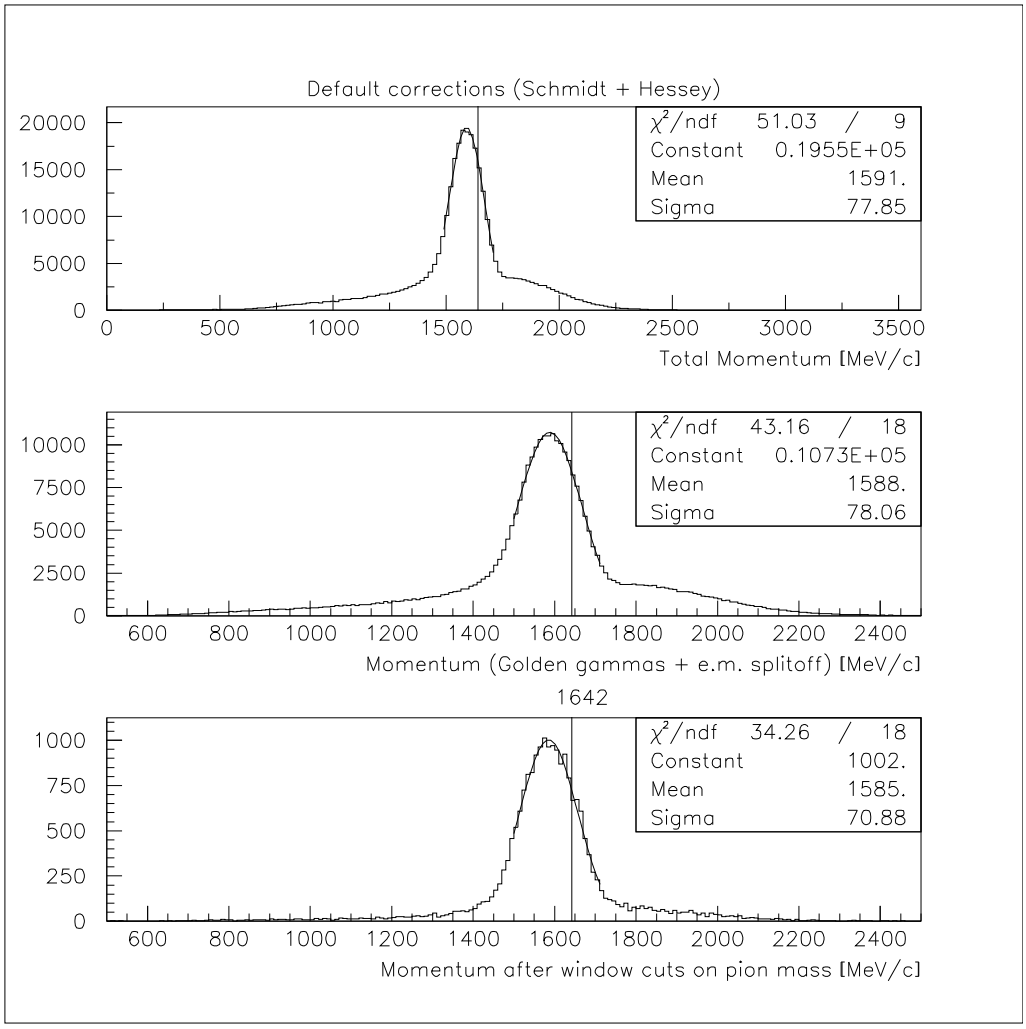

Figure 9: Total momentum distribution

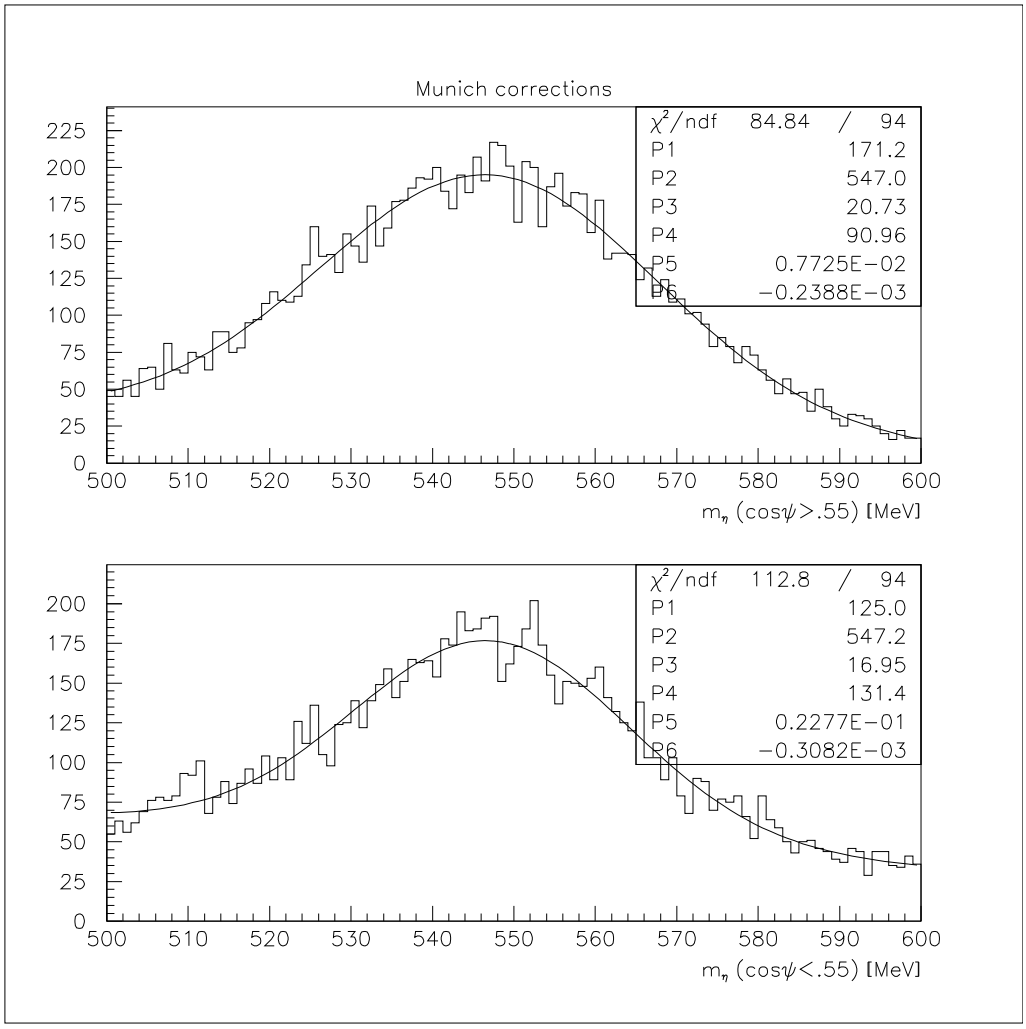

Figure 10: Invariant η mass at different ranges of the decaying angle

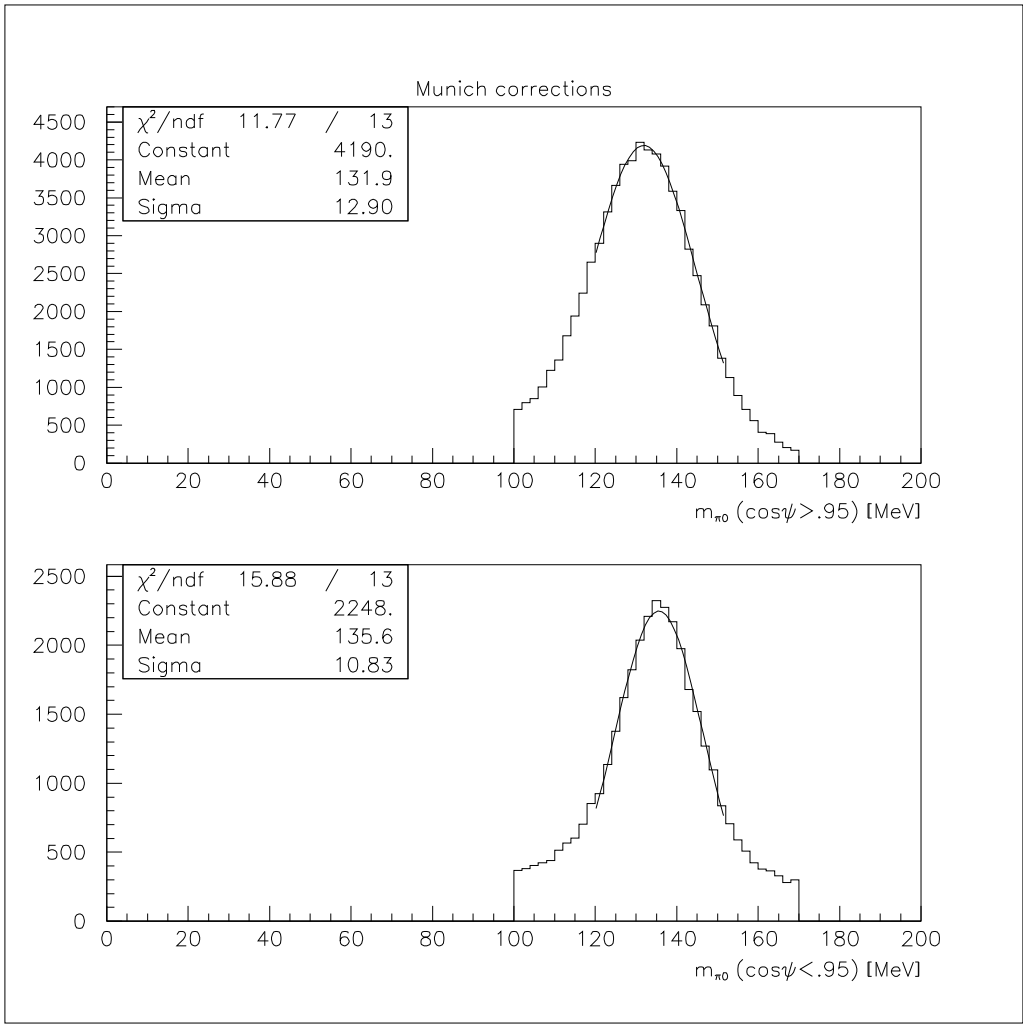

Figure 11: Invariant π^0 mass at different ranges of the decaying angle

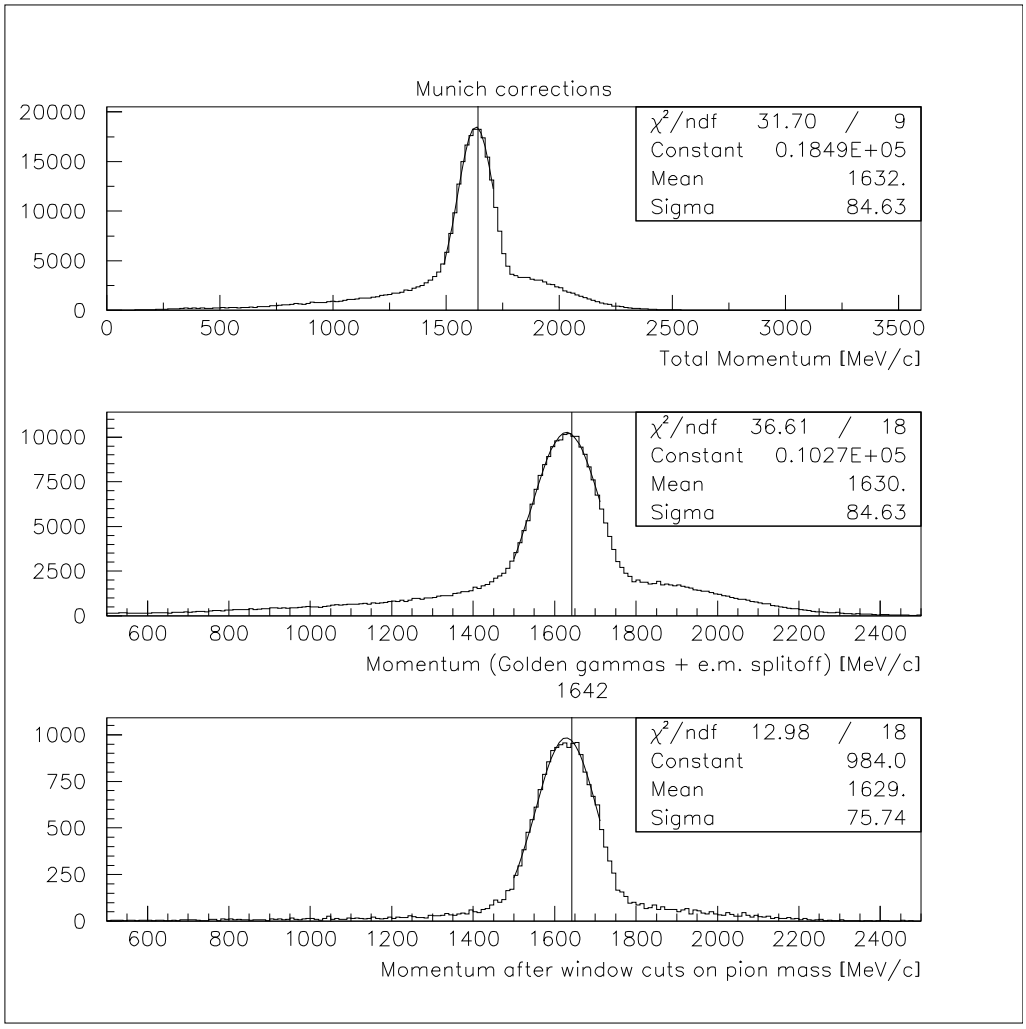

Figure 12: Total momentum distribution

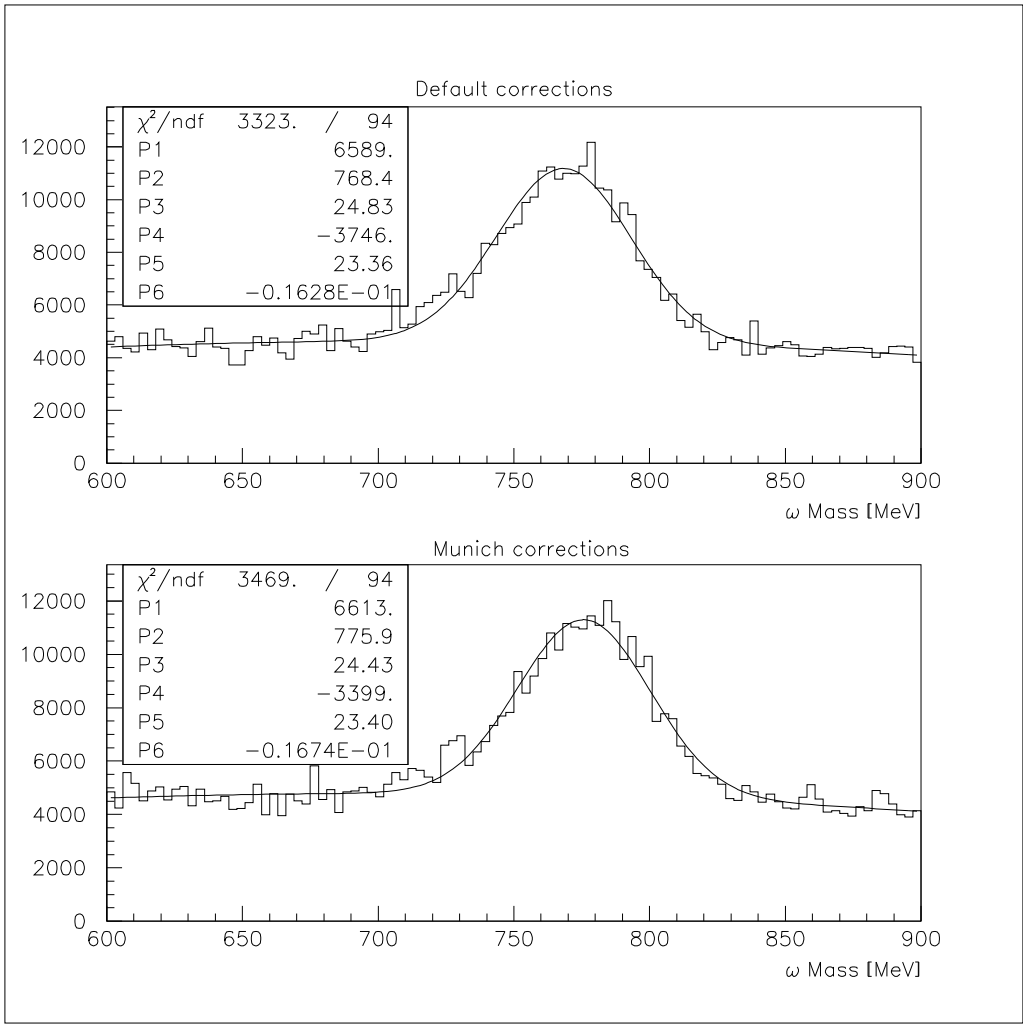

Figure 13: $\omega \to \pi^0\gamma$ invariant mass

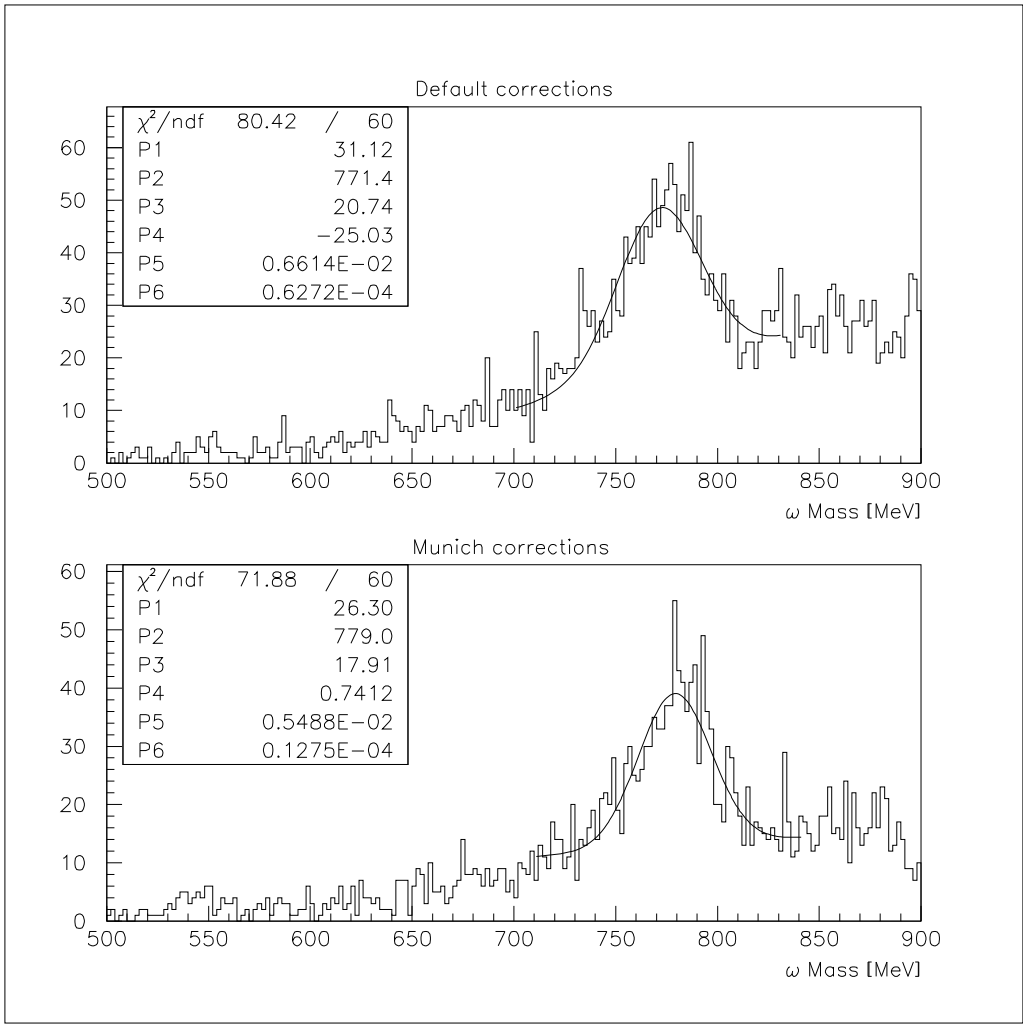

Figure 14: $\omega \to \pi^+\pi^-\pi^0$ invariant mass

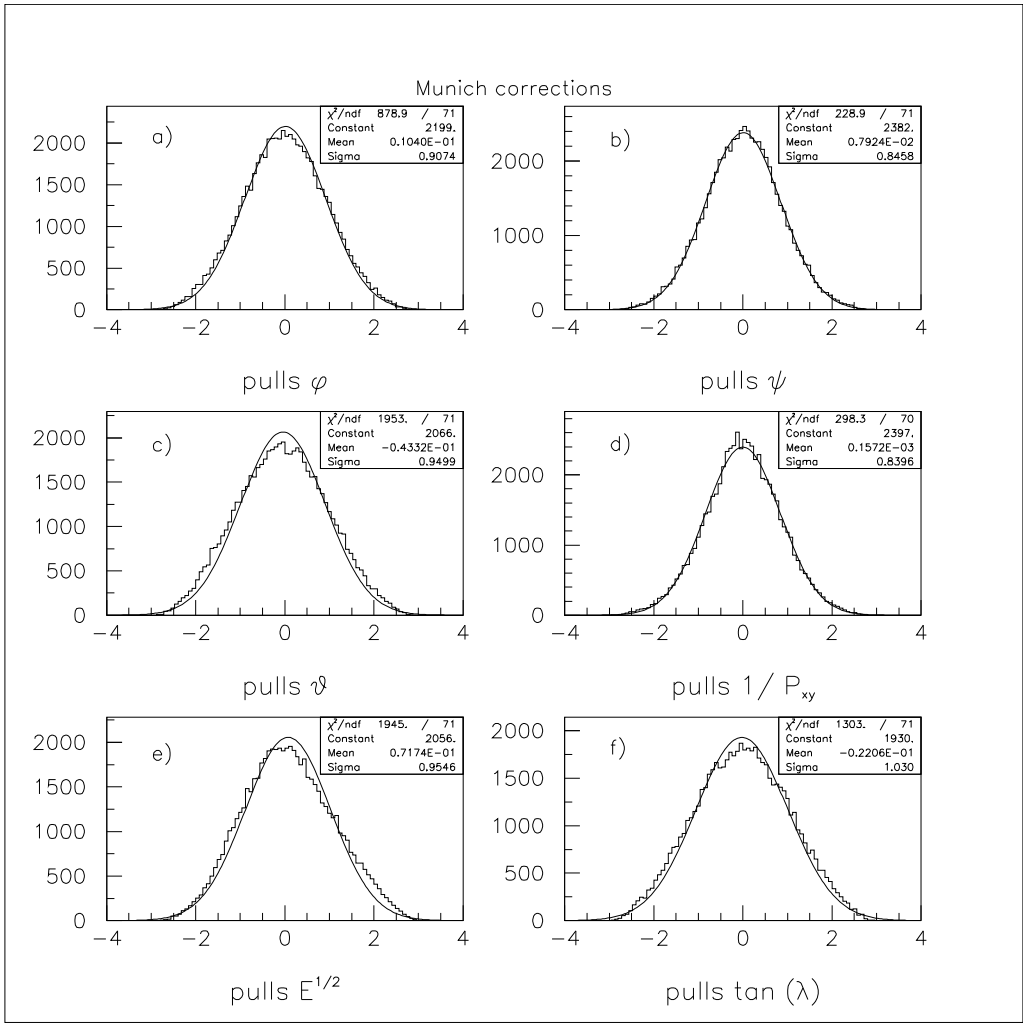

Figure 15: Pulls for $\bar{p}p \to K^+K^-\pi^0$ Events at 900 MeV/c

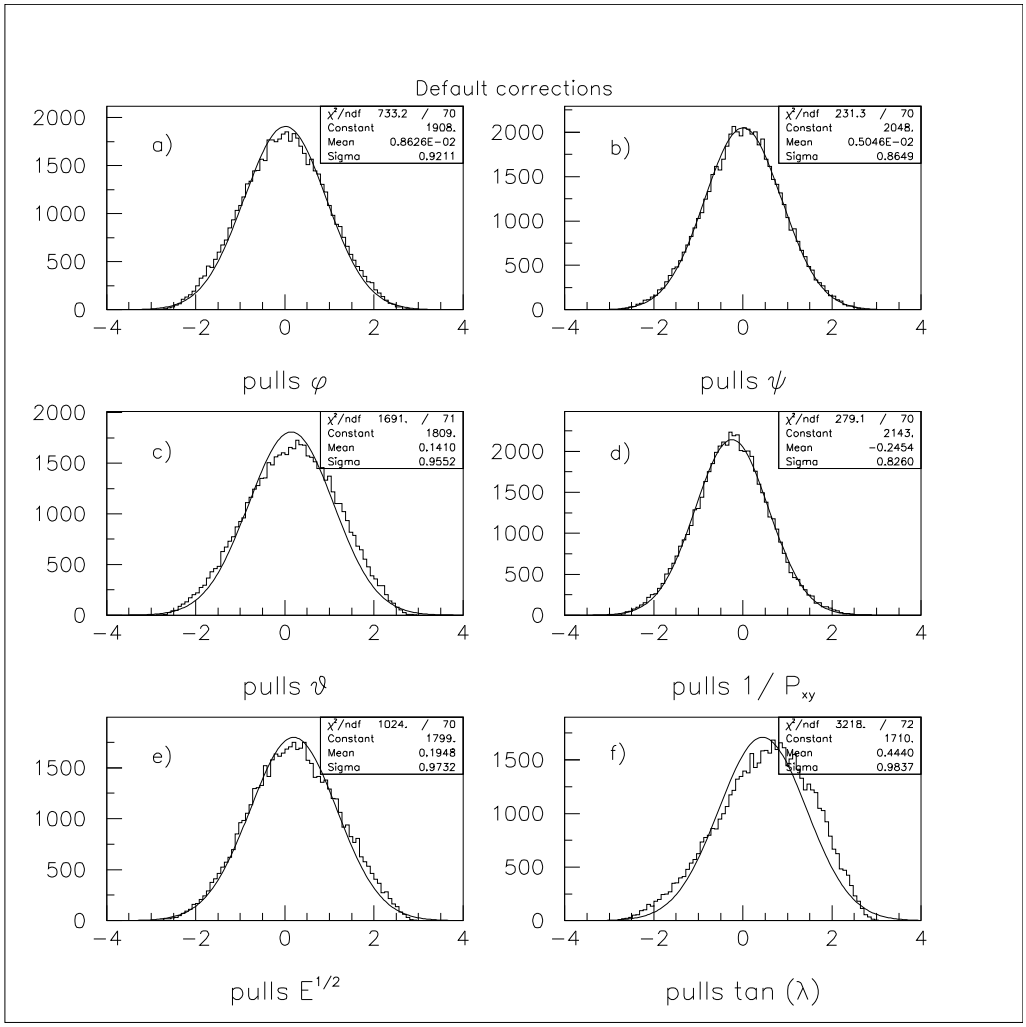

Figure 16: Pulls for $\bar{p}p \to K^+K^-\pi^0$ Events at 900 MeV/c